

# Inflationary potentials in DBI models

Dennis Bessada<sup>1,2,\*</sup>, William H. Kinney<sup>1,†</sup>, and Konstantinos Tzirakis<sup>1,‡</sup>

<sup>1</sup>*Dept. of Physics, University at Buffalo, the State University of New York, Buffalo, NY 14260-1500, United States*

<sup>2</sup>*INPE - Instituto Nacional de Pesquisas Espaciais - Divisão de Astrofísica, São José dos Campos, 12227-010 SP, Brazil*

(Dated: January 9, 2019)

We study DBI inflation based upon a general model characterized by a power-law flow parameter  $\epsilon(\phi) \propto \phi^\alpha$  and speed of sound  $c_s(\phi) \propto \phi^\beta$ , where  $\alpha$  and  $\beta$  are constants. We show that in the slow-roll limit this general model gives rise to distinct inflationary classes according to the relation between  $\alpha$  and  $\beta$  and to the time evolution of the inflaton field, each one corresponding to a specific potential; in particular, we find that the well-known canonical polynomial (large- and small-field), hybrid and exponential potentials also arise in this non-canonical model. We find that these non-canonical classes have the same physical features as their canonical analogs, except for the fact that the inflaton field evolves with varying speed of sound; also, we show that a broad class of canonical and D-brane inflation models are particular cases of this general non-canonical model. Next, we compare the predictions of large-field polynomial models with the current observational data, showing that models with low speed of sound have red-tilted scalar spectrum with low tensor-to-scalar ratio, in good agreement with the observed values. These models also show a correlation between large non-gaussianity with low tensor amplitudes, which is a distinct signature of DBI inflation with large-field polynomial potentials.

PACS numbers: 98.80.Cq

## I. INTRODUCTION

With the advent of the Five-year WMAP data [1] the inflationary paradigm [2, 3, 4, 5] (henceforth called *canonical inflation*) has been confirmed as the most successful candidate for explaining the physics of the very early universe [6]. The very rapid acceleration period generated by canonical inflation has solved some of the puzzles of the standard cosmological model, such as the horizon, flatness and entropy problems. However, existing models for inflation are phenomenological in character, and a fundamental explanation of inflation is still missing. Also, the scalar field responsible for the inflationary expansion - the *inflaton* - is generically highly fine-tuned.

Over the past few years developments in string theory have shed new light on these two problems of canonical inflation. String theory predicts a broad class of scalar fields associated with the compactification of extra dimensions and the configuration of lower-dimensional branes moving in a higher-dimensional bulk space. This fact gave rise to some phenomenologically viable inflation models, such as the KKLTMMT scenario [7], Racetrack Inflation [8], Roulette Inflation [9], and the Dirac-Born-Infeld (DBI) scenario [10]. In particular, from a phenomenological point of view, the DBI scenario has a very interesting and far-reaching feature: being a special case of a larger class of inflationary models with non-canonical Lagrangians called *k-inflation* [11], the DBI model possesses a varying speed of sound. This is a far-reaching

feature because, in this case, slow-roll can be achieved via a low sound speed instead of from dynamical friction due to expansion which, in turn, leads to substantial non-Gaussianity [12, 13, 14, 15, 16]. Also, DBI inflation admits several exact solutions to the flow equations (first introduced in [17] for the canonical case, and generalized in [18] for DBI inflation), as discussed in [14, 19, 20, 21, 22].

In this paper we derive a family of non-canonical models characterized by a power-law in the inflaton field  $\phi$  for the speed of sound  $c_s$  and the flow parameter  $\epsilon$ . We then derive the forms of the associated inflationary potentials, and group them according to the classification scheme introduced in Ref. [23], in order to have a better physical picture of the solutions obtained. We later show that some particular cases possess spectral indices in agreement with the current observational values, and establish the limits for the speed of sound in order that their tensor-to-scalar ratio correspond to the observed values. The outline of the paper is as follows: in section II we review the DBI inflation and the flow formalism for non-canonical inflation with time-varying speed of sound. In section III we review the tools needed to calculate the scalar and tensor spectral indices for slow-roll. In section IV we introduce the main features of our model and derive general solutions, postponing the discussion of their physical properties to section V, where we extend the concept of large-field, small-field, hybrid and exponential potentials of canonical inflation to the non-canonical case. In section VI we compare the observational predictions of a set of non-canonical large-field models with WMAP5 data, and show that there is a generic correlation between small sound speed (and therefore significant non-Gaussianity) and a low tensor/scalar ratio. We present conclusions in VII.

\*dbessada@buffalo.edu,

†whkinney@buffalo.edu,

‡ct38@buffalo.edu

## II. DBI INFLATION - AN OVERVIEW

In warped D-brane inflation (see [24] and [25] for a review), inflation is regarded as the motion of a D3-brane in a six-dimensional “throat” characterized by the metric [26]

$$ds_{10}^2 = h^2(r) ds_4^2 + h^{-2}(r) (dr^2 + r^2 ds_{X_5}^2), \quad (1)$$

where  $h$  is the warp factor,  $X_5$  is a Sasaki-Einstein five-manifold which forms the base of the cone, and  $r$  is the radial coordinate along the throat. In this case, the inflaton field  $\phi$  is identified with  $r$  as  $\phi = \sqrt{T_3} r$ , where  $T_3$  is the brane tension. The dynamics of the D3-brane in the warped background (1) is then dictated by the DBI Lagrangian

$$\mathcal{L} = -f^{-1}(\phi) \sqrt{1 - 2f(\phi) X} - f^{-1}(\phi) - V(\phi), \quad (2)$$

where  $g_{\mu\nu}$  is the background spacetime metric,  $f^{-1}(\phi) = T_3 h(\phi)^4$  is the inverse brane tension,  $V(\phi)$  is an arbitrary potential, and  $X = (1/2)g^{\mu\nu} \partial_\mu \phi \partial_\nu \phi$  is the kinetic term. We assume that the background cosmological model is described by the flat Friedmann-Robertson-Walker (FRW) metric,  $g_{\mu\nu} = \text{diag}\{1, -a^2(t), -a^2(t), -a^2(t)\}$ . DBI inflation is a special case of *k-inflation*, characterized by a varying speed of sound  $c_s$ , whose expression is given by

$$c_s^2 = \left(1 + 2X \frac{\mathcal{L}_{,XX}}{\mathcal{L}_{,X}}\right)^{-1}, \quad (3)$$

where the subscript “ $X$ ” indicates a derivative with respect to the kinetic term. It is straightforward to see that in the model (2) the speed of sound is given by

$$c_s(\phi) = \sqrt{1 - 2f(\phi)X}. \quad (4)$$

In those models it is convenient to introduce an analog of the Lorentz factor, related to  $c_s(\phi)$  by:

$$\gamma(\phi) = \frac{1}{c_s(\phi)}. \quad (5)$$

We next introduce the generalization of the inflationary flow hierarchy for *k-inflation* models [18]. The two fundamental flow parameters are

$$\epsilon(\phi) = \frac{2M_P^2}{\gamma(\phi)} \left( \frac{H'(\phi)}{H(\phi)} \right)^2, \quad (6a)$$

$$s(\phi) = \frac{2M_P^2}{\gamma(\phi)} \frac{H'(\phi)}{H(\phi)} \frac{\gamma'(\phi)}{\gamma(\phi)}, \quad (6b)$$

where the prime indicates a derivative with respect to  $\phi$ . An infinite hierarchy of additional flow parameters can be generated by differentiation, and are defined as follows:

$$\eta(\phi) = \frac{2M_P^2}{\gamma(\phi)} \frac{H''(\phi)}{H(\phi)},$$

$$\begin{aligned} & \vdots \\ {}^\ell \lambda(\phi) &= \left( \frac{2M_P^2}{\gamma(\phi)} \right)^\ell \left( \frac{H'(\phi)}{H(\phi)} \right)^{\ell-1} \frac{1}{H(\phi)} \frac{d^{\ell+1} H(\phi)}{d\phi^{\ell+1}}, \\ \rho(\phi) &= \frac{2M_P^2}{\gamma(\phi)} \frac{\gamma''(\phi)}{\gamma(\phi)}, \\ & \vdots \\ {}^\ell \alpha(\phi) &= \left( \frac{2M_P^2}{\gamma(\phi)} \right)^\ell \left( \frac{H'(\phi)}{H(\phi)} \right)^{\ell-1} \frac{1}{\gamma(\phi)} \frac{d^{\ell+1} \gamma(\phi)}{d\phi^{\ell+1}}, \end{aligned} \quad (7)$$

where  $\ell = 2, \dots, \infty$  is an integer index. It is convenient to express the flow parameters (7) in terms of the number of e-folds before the end of inflation, which is defined in the following way:

$$N = - \int H dt = \frac{1}{\sqrt{2M_P^2}} \int_{\phi_e}^{\phi} \sqrt{\frac{\gamma(\phi)}{\epsilon(\phi)}} d\phi, \quad (8)$$

where  $\phi_e$  indicates the value of the inflaton field at the end of inflation. The definition above indicates that the number of e-folds increases as we go backward in time, so that it is zero at the end of inflation. We can also determine the scale factor,  $a$ , in terms of  $N$  in a straightforward way: since  $da/a = dtH = -dN$ , we simply have

$$a(N) = a_e e^{-N}. \quad (9)$$

In terms of  $N$ , it is easy to see that the key flow parameters  $\epsilon$  and  $s$ , as defined in (6a) and (6b), assume the following equivalent form

$$\epsilon = \frac{1}{H} \frac{dH}{dN}, \quad (10a)$$

$$s = \frac{1}{\gamma} \frac{d\gamma}{dN}, \quad (10b)$$

so that we may derive a set of first-order differential equations

$$\begin{aligned} \frac{d\epsilon}{dN} &= \epsilon(2\eta - 2\epsilon - s), \\ \frac{d\eta}{dN} &= -\eta(\epsilon + s) + {}^2\lambda, \\ &\vdots \\ \frac{d^\ell \lambda}{dN} &= -{}^\ell \lambda [\ell(s + \epsilon) - (\ell - 1)\eta] + {}^{\ell+1}\lambda, \\ \frac{ds}{dN} &= -s(2s + \epsilon - \eta) + \epsilon\rho, \\ \frac{d\rho}{dN} &= -2\rho s + {}^2\alpha, \\ &\vdots \\ \frac{d^\ell \alpha}{dN} &= -{}^\ell \alpha [(\ell + 1)s + (\ell - 1)(\epsilon - \eta)] + {}^{\ell+1}\alpha. \end{aligned} \quad (11)$$

The dynamics of the inflaton field can be completely described by this hierarchy of equations, which are equivalent to the Hamilton-Jacobi equations [27]

$$\dot{\phi} = -\frac{2M_P^2}{\gamma(\phi)} H'(\phi), \quad (12a)$$

$$3M_P^2 H^2(\phi) - V(\phi) = \frac{\gamma(\phi) - 1}{f(\phi)}, \quad (12b)$$

where  $M_P = 1/\sqrt{8\pi G}$  is the reduced Planck mass, and

$$\gamma(\phi) = \sqrt{1 + 4M_P^4 f(\phi) [H'(\phi)]^2}. \quad (13)$$

In terms of the flow parameter  $\epsilon$ , the potential,  $V(\phi)$ , and the inverse brane tension,  $f(\phi)$ , can be written as

$$V(\phi) = 3M_P^2 H^2 \left(1 - \frac{2\epsilon}{3} \frac{\gamma}{\gamma + 1}\right), \quad (14)$$

and

$$f(\phi) = \frac{1}{2M_P^2 H^2 \epsilon} \left(\frac{\gamma^2 - 1}{\gamma}\right), \quad (15)$$

respectively. Our strategy in this paper is to generate inflationary solutions by *ansatz* for the flow parameters  $\epsilon$  and  $s$ , for which the forms of the functions  $V(\phi)$  and  $f(\phi)$  are determined.

In the next section, we briefly review the generation of perturbations in non-canonical inflation models.

### III. POWER SPECTRA

Scalar and tensor perturbations in k-inflation were first studied in Ref. [28], where it was shown that the quantum mode function  $u_k$  obeys the equation of motion

$$u_k'' + \left(c_s^2 k^2 - \frac{z''}{z}\right) u_k = 0, \quad (16)$$

where  $k$  is the comoving wave number, a prime denotes a derivative with respect to conformal time  $d\tau \equiv dt/a$ , and  $z$  is a variable given by

$$z = \frac{a\sqrt{\rho+p}}{c_s H} = \frac{a\gamma^{3/2}\dot{\phi}}{H} = -M_P a\gamma\sqrt{2\epsilon}. \quad (17)$$

It is convenient to change the conformal time,  $\tau$ , to

$$y \equiv \frac{k}{\gamma a H}, \quad (18)$$

so that

$$\frac{d^2}{d\tau^2} = a^2 H^2 \left[ (1 - \epsilon - s)^2 y^2 \frac{d^2}{dy^2} + G(\epsilon, \eta, s, \rho) y \frac{d}{dy} \right], \quad (19)$$

where

$$G = -s + 3\epsilon s - 2\epsilon\eta - \eta s + 2\epsilon^2 + 3s^2 - \epsilon\rho. \quad (20)$$

We can also show that

$$\frac{z''}{z} = a^2 H^2 F(\epsilon, \eta, s, \rho, {}^2\lambda), \quad (21)$$

where [29]

$$F = 2 + 2\epsilon - 3\eta - \frac{3}{2}s - 4\epsilon\eta + \frac{1}{2}\eta s + 2\epsilon^2$$

$$+ \eta^2 - \frac{3}{4}s^2 + {}^2\lambda + \frac{1}{2}\epsilon\rho. \quad (22)$$

Substituting (19) and (21) into (16), we find

$$(1 - \epsilon - s)^2 y^2 \frac{d^2 u_k}{dy^2} + G y \frac{du_k}{dy} + [y^2 - F] u_k = 0, \quad (23)$$

which is an exact equation, without any assumption of slow-roll.

We now proceed to solve equation (23) to first-order in slow-roll. In this case, this equation takes the form

$$(1 - 2\epsilon - 2s) y^2 \frac{d^2 u_k}{dy^2} - s y \frac{du_k}{dy} + \left[ y^2 - 2(1 + \epsilon - \frac{3}{2}\eta - \frac{3}{4}s) \right] u_k = 0, \quad (24)$$

whose solution is [21]

$$u_k(y) = \frac{1}{2} \sqrt{\frac{\pi}{c_s k}} \sqrt{\frac{y}{1 - \epsilon - s}} H_\nu \left( \frac{y}{1 - \epsilon - s} \right), \quad (25)$$

where  $H_\nu$  is a Hankel function, and

$$\nu = \frac{3}{2} + 2\epsilon - \eta + s. \quad (26)$$

The power spectra for scalar and tensor perturbations are given respectively by

$$\begin{aligned} P_{\mathcal{R}} &= \frac{1}{8\pi^2} \left. \frac{H^2}{M_P^2 c_s \epsilon} \right|_{c_s k = aH}, \\ P_T &= \frac{2}{\pi^2} \left. \frac{H^2}{M_P^2} \right|_{k = aH}, \end{aligned} \quad (27)$$

so that, for the solution (25),

$$\begin{aligned} P_{\mathcal{R}}^{1/2} &= [(1 - \epsilon - s) \\ &\quad + (2 - \ln 2 - \gamma)(2\epsilon - \eta + s)] \left. \frac{H^2}{2\pi\dot{\phi}} \right|_{k=\gamma aH} \end{aligned} \quad (28)$$

where  $\gamma \approx 0.577$  is Euler's constant. From the definitions of the scalar and tensor spectral indices,

$$\begin{aligned} n_s - 1 &\equiv \frac{d(\ln P_{\mathcal{R}})}{d(\ln k)}, \\ n_T &\equiv \frac{d(\ln P_T)}{d(\ln k)}, \end{aligned} \quad (29)$$

we find

$$\begin{aligned} n_s - 1 &= -4\epsilon + 2\eta - 2s, \\ n_T &= -2\epsilon, \end{aligned} \quad (30)$$

valid to first-order in the slow-roll limit. The tensor-to-scalar ratio is then given by

$$r = \frac{P_T}{P_{\mathcal{R}}} = 16c_s \epsilon, \quad (31)$$

which is valid in the general k-inflation case [28]. It is immediately clear from this expression that small  $c_s$  has the generic effect of suppressing the tensor/scalar ratio.

## IV. THE MODEL

### A. The General Setting

The usual approach to the construction of a model of inflation normally starts with a choice of the inflaton potential,  $V(\phi)$ ; then, all the flow parameters are derived, and the dynamical analysis is performed. In this work we adopt the reverse procedure: we first look for the solutions to the differential equation satisfied by the Hubble parameter  $H(\phi)$ ,

$$\frac{H'(\phi)}{H(\phi)} = \pm \sqrt{\frac{\epsilon(\phi)\gamma(\phi)}{2M_P^2}}, \quad (32)$$

and only afterwards derive the form of the potential. Equation (32) can be easily derived from the definition of the flow parameter  $\epsilon$ , given by (6a), and the sign ambiguity indicates in which direction the field is rolling. Notice that in order to solve equation (32) we must know the form of the functions  $\epsilon(\phi)$  and  $\gamma(\phi)$ ; we choose them to be power-law functions of the inflaton field,

$$\epsilon(\phi) = \left(\frac{\phi}{\phi_e}\right)^\alpha, \quad (33a)$$

$$\gamma(\phi) = \gamma_e \left(\frac{\phi}{\phi_e}\right)^\beta, \quad (33b)$$

where  $\gamma_e$  is the value of the Lorentz factor at the end of inflation<sup>1</sup>, and  $\alpha$  and  $\beta$  are constants. Another case worth studying appears when  $\epsilon$  is *constant*, so that

$$\epsilon(\phi) = \epsilon = \text{const.}, \quad (34)$$

with the same parametrization for  $\gamma$ . We have kept  $\phi_e$  for the following reason: in the *IR* DBI model the inflaton field rolls down from the tip of the throat toward the bulk of the manifold with increasing speed of sound; then, when the field enters the bulk  $c_s$  becomes equal to 1, and then inflation “ends”. In the *UV* case the behavior is the opposite, that is, the field evolves away from the bulk and reaches the tip when  $c_s = 1$ . To reproduce both cases we could have set  $\gamma_e = 1$  from the onset, so that  $c_s(\phi_e) = 1$ , as required; also,  $c_s(\phi) = 1$  in the canonical limit, that is, when  $\beta = 0$ . However, by taking  $\gamma_e$  arbitrary, we also reproduce the non-canonical models with constant speed of sound introduced by Spalinski [20]. It is clear that in the latter case  $\gamma_e$  does not refer necessarily to the end of inflation, so that if we take  $\gamma_e \gg 1$  it does not mean a superluminal propagation (as would be the case if  $\beta \neq 0$ ). Bearing this distinction in mind we can use the same notation unambiguously.

When  $\alpha \neq 0$ , substituting (33a) and (33b) into (32), we see that the Hubble parameter takes the form

$$H(\phi) = H_e \exp \left[ \sigma \sqrt{\frac{\gamma_e}{2M_P^2 \phi_e^{\alpha+\beta}}} I(\phi) \right], \quad (35)$$

where we have defined

$$I(\phi) \equiv \int_{\phi_e}^{\phi} d\phi' \phi'^{(\alpha+\beta)/2}, \quad (36)$$

and  $\sigma$  accounts for the sign ambiguity appearing in (32). When  $\epsilon$  is constant, the solution to (32) reads

$$H(\phi) = H_e \exp \left[ \sigma \sqrt{\frac{\epsilon \gamma_e}{2M_P^{\beta+2}}} I(\phi) \right], \quad (37)$$

where the integral  $I(\phi)$  is the same as in (36).

It is clear that the integral (36) admits two distinct solutions: a logarithmic one when  $\alpha+\beta = -2$ , and power-law for  $\alpha+\beta \neq -2$ . These two solutions will give rise to different classes of inflationary potentials, which we shall address in the next subsections.

To conclude this section we derive the general formula for the number of e-folds. For  $\alpha \neq 0$  this expression can be determined by equations (8), (33a), and (33b), so that

$$N(\phi) = \sigma \sqrt{\frac{\gamma_e \phi_e^{\alpha-\beta}}{2M_P^2}} J(\phi), \quad (38)$$

where

$$J(\phi) = \int_{\phi_e}^{\phi} d\phi' \phi'^{(\beta-\alpha)/2}; \quad (39)$$

if  $\alpha = 0$  we must use the parametrization (34), so that expression (38) changes to

$$N(\phi) = \sigma \sqrt{\frac{\gamma_e}{2M_P^2 \epsilon \phi_e^\beta}} \tilde{J}(\phi), \quad (40)$$

where

$$\tilde{J}(\phi) = \int_{\phi_e}^{\phi} d\phi' \phi'^{\beta/2}. \quad (41)$$

In the next section, we discuss particular cases of this general class of solutions.

### B. The Solutions $\alpha + \beta = -2$ .

For this class of solutions, the parameters  $\alpha$  and  $\beta$  are related by

$$\alpha = -2 - \beta; \quad (42)$$

<sup>1</sup> Henceforth all the variables with a subscript  $e$  are evaluated at the end of inflation.

notice that the case  $\alpha = 0$  implies  $\beta = -2$ , which corresponds to the case where the flow parameters  $\epsilon$  and  $s$  are constant [21]. Evaluating the integral (36) and substituting it into (35), we find

$$H(\phi) = H_e \left( \frac{\phi}{\phi_e} \right)^{p/2}, \quad (43)$$

where the exponent  $p$  is determined by

$$p = \sigma \phi_e \sqrt{\frac{2\gamma_e}{M_P^2}}. \quad (44)$$

Let us now analyze the sign ambiguity appearing in (44). We first write the expression (43) as

$$p = 2 \frac{\ln(H(\phi)/H_e)}{\ln(\phi/\phi_e)}; \quad (45)$$

then, for  $\alpha < 0$ , we have, from (33a), in the slow-roll limit,

$$\epsilon(\phi) = \left( \frac{\phi}{\phi_e} \right)^{-|\alpha|} \ll 1, \quad (46)$$

which implies  $\phi \gg \phi_e$  and  $\dot{\phi} < 0$  for  $\phi > 0$  (*large-field limit*), so that  $\ln(\phi/\phi_e) > 0$ . Since the weak-energy condition implies that  $\dot{H} < 0$ , we have  $H(\phi) \geq H_e$ , and then  $\ln(H(\phi)/H_e) > 0$ . Therefore, from (45),  $\alpha < 0$  implies  $p > 0$ . From definition (44) we see that  $p > 0$  implies  $\sigma = -1$  if  $\phi < 0$ , and  $\sigma = +1$  if  $\phi > 0$ .

Conversely, if  $\alpha > 0$ , we have, from (33a), in the slow-roll limit,

$$\epsilon(\phi) = \left( \frac{\phi}{\phi_e} \right)^{+|\alpha|} \ll 1, \quad (47)$$

which implies  $\phi \ll \phi_e$  and  $\dot{\phi} > 0$  for  $\phi > 0$  (*small-field limit*), so that  $\ln(\phi/\phi_e) < 0$ . Again,  $\ln(H(\phi)/H_e) > 0$ , so that, from (45),  $\alpha > 0$  implies  $p < 0$ . From definition (44) we see that  $p < 0$  implies  $\sigma = -1$  if  $\phi > 0$ , and  $\sigma = +1$  if  $\phi < 0$ .

Therefore, what really distinguishes the models is the sign of the exponent of  $\alpha$ ; the sign of  $\sigma$  simply dictates which direction the field is rolling in, exactly as in canonical inflation. We are left with two distinct models, whose properties are summarized in Table I. (For  $\phi < 0$  the

TABLE I: The sign rule for models with  $\alpha + \beta = -2$  and  $\phi > 0$ .

Model 1.	$p > 0, \alpha < 0$	$\sigma = +1$	$\phi > 0$	$\dot{\phi} < 0$
Model 2.	$p < 0, \alpha > 0$	$\sigma = +1$	$\phi > 0$	$\dot{\phi} < 0$

sign rule is easily obtained by flipping all the signs of the quantities present in Table I.)

### C. The Solutions $\alpha + \beta \neq -2$

Let us first consider the case  $\alpha \neq 0$ . The solution to the integral (36) is

$$H(\phi) = \tilde{H}_e \exp \left[ \frac{\sigma K \phi_e}{\alpha + \beta + 2} \bar{\phi}^{(\alpha+\beta+2)/2} \right], \quad (48)$$

where we have defined

$$\tilde{H}_e = H_e \exp \left[ -\frac{\sigma \sqrt{2\gamma_e} \phi_e}{M_P(\alpha + \beta + 2)} \right], \quad (49)$$

$$K = \sqrt{\frac{2\gamma_e}{M_P^2}}, \quad \bar{\phi} = \frac{\phi}{\phi_e}. \quad (50)$$

In order to fix the sign ambiguity let us rewrite expression (48) as

$$d \ln H = \frac{2\sigma K \phi_e}{\alpha + \beta + 2} d\bar{\phi}^{(\alpha+\beta+2)/2}; \quad (51)$$

then, as we have seen in (46), the condition  $\alpha < 0$  corresponds to the large-field limit,  $\phi \gg \phi_e$ ; so, if  $\alpha + \beta + 2 < 0$  and  $\phi > 0$ , we have  $d\bar{\phi}^{(\alpha+\beta+2)/2} > 0$ , so that from (51),

$$\underbrace{d \ln H}_{<0} = \frac{2\sigma K \phi_e}{\alpha + \beta + 2} \underbrace{d\bar{\phi}^{(\alpha+\beta+2)/2}}_{>0} \Rightarrow -\frac{\sigma K |\phi_e|}{|\alpha + \beta + 2|} < 0, \quad (52)$$

implying that  $\sigma = +1$ . Applying the same analysis for  $\alpha + \beta + 2 < 0$  and  $\phi < 0$ , we find  $\sigma = -1$ . For  $\alpha + \beta + 2 > 0$  we find  $\sigma = +1$  for  $\phi > 0$ , and  $\sigma = -1$  for  $\phi < 0$ . The results in the large-field limit are summarized in Table II. The same reasoning also applies for  $\alpha > 0$ , that is, the small-field limit, given by (47); the results are summarized in Table III, where we have four distinct models: As in the previous case, the model  $\phi < 0$  is

TABLE II: The sign rule for models with  $\alpha + \beta \neq -2$ ,  $\alpha < 0$ , and  $\phi > 0$ .

Model 3.	$\alpha + \beta + 2 > 0$	$\sigma = +1$	$\dot{\phi} < 0$
Model 4.	$\alpha + \beta + 2 < 0$	$\sigma = +1$	$\dot{\phi} < 0$

TABLE III: The sign rule for models with  $\alpha + \beta \neq 0$ ,  $\alpha > 0$  and  $\phi > 0$ .

Model 5.	$\alpha + \beta + 2 > 0$	$\sigma = -1$	$\dot{\phi} > 0$
Model 6.	$\alpha + \beta + 2 > 0$	$\sigma = +1$	$\dot{\phi} < 0$
Model 7.	$\alpha + \beta + 2 < 0$	$\sigma = -1$	$\dot{\phi} > 0$
Model 8.	$\alpha + \beta + 2 < 0$	$\sigma = +1$	$\dot{\phi} < 0$

easily obtained by flipping all the signs of the quantities present in Tables II and III.



In the case  $\epsilon = \text{const.}$ ,  $\beta \neq -2$ , the solution to the integral (36) is given by

$$H(\phi) = \tilde{H}_e \exp \left[ \sigma \sqrt{\frac{2\epsilon\gamma_e}{M_P^2\phi_e^\beta}} \frac{\phi^{(\beta+2)/2}}{\beta+2} \right], \quad (53)$$

where

$$\tilde{H}_e = H_e \exp \left[ -\sigma \sqrt{\frac{2\epsilon\gamma_e}{M_P^2\phi_e^\beta}} \frac{\phi_e^{(\beta+2)/2}}{\alpha+\beta+2} \right]. \quad (54)$$

It is straightforward to see that the same sign rules shown in Tables II and III also apply to this case.

## V. CLASSES OF INFLATIONARY POTENTIALS IN DBI INFLATION

In this section we proceed to analyze the solutions obtained in the last section. The key ingredient, in order to understand the physics associated with these classes of solutions, is the study of the form of the inflationary potential, which is obtained from the expressions (14), (33b), and the corresponding expression for the Hubble parameter, given by either (43) or (48). Once we have the form of such non-canonical potentials, we can compare these expressions with the usual canonical inflationary potentials, grouped into four general classes: the *large-* and *small-field polynomial*, *hybrid*, and *exponential* models [23]. To do so, we must make some choices for the exponents  $\alpha$  and  $\beta$  first, and then on the corresponding dynamics of the field; hence, as we have seen in the tables I, II and III, we have eight distinct models altogether. Our main aim is to reproduce the classes of the inflationary potentials discussed in [23]; then, in doing so, we leave out some interesting solutions, but our emphasis here is on understanding the physics of the non-canonical models, which can be achieved through a close comparison with the well-established potentials found in the literature.

### A. Large-field polynomial potentials

In these models, the inflaton field is displaced far from its minimum to a value  $\phi \sim \mu$ , and then rolls down toward its minimum at the origin on a potential  $V(\phi) \propto \phi^p$ . A quick look at expressions (14) and (43) suggests that the model 1 in table I, characterized by  $p > 0$  and  $\alpha < 0$ , is its non-canonical counterpart, for its potential also goes like  $\phi^p$ . To check this, let us first analyze the behavior of the speed of sound (33b). Since the equality (42) implies  $\beta > -2$ , we see from (33b) that  $\beta > 0$  corresponds to

$$\gamma(\phi) = \gamma_e \left( \frac{\phi}{\phi_e} \right)^{|\beta|} \implies \gamma \rightarrow \infty \quad \text{as} \quad \phi \rightarrow \infty, \quad (55)$$

or, in terms of the speed of sound,

$$c_s \rightarrow 0 \quad \text{as} \quad \phi \rightarrow \infty; \quad (56)$$

since in the large-field limit the field strength is very large at early times, we conclude from (56) that the speed of sound starts off with a *subluminal* value. Also, from (55), we see that  $\gamma/(\gamma+1) \rightarrow 1$ ; then, using this fact and plugging (43) into (14), we find

$$V(\phi) \sim 3M_P^2 H_e^2 \left( \frac{\phi}{\phi_e} \right)^p, \quad (57)$$

which has exactly the same form of a canonical large-field potential. The non-canonical potential (57) shows that the inflaton field starts evolving from a value  $\phi \sim \mu$  with a very low speed of sound, and then rolls down toward its minimum at origin. Once there, the speed of sound becomes unity as well as the flow parameter  $\epsilon$  and then inflation ends. The potential evaluated at  $\mu$  corresponds to the vacuum energy density,

$$V(\mu) = \Lambda^4 \implies \Lambda^4 \sim 3M_P^2 H_e^2, \quad (58)$$

so that in terms of these two quantities, the Hubble parameter (43) and the inflationary potential (57) assume the form

$$H(\phi) = \frac{\Lambda^2}{\sqrt{3M_P^2}} \left( \frac{\phi}{\mu} \right)^{p/2} \quad (59)$$

$$V(\phi) = \Lambda^4 \left( \frac{\phi}{\mu} \right)^p, \quad (60)$$

respectively.

The end of inflation is achieved when  $\phi = \phi_e$ , whose value can be determined from (44) and the sign rule for the model 1 in table I:

$$\frac{\phi_e}{M_P} = \frac{p}{\sqrt{2\gamma_e}}; \quad (61)$$

then, in terms of the expression (61) the flow parameter  $\epsilon$  takes the form

$$\epsilon(\phi) = \left[ \frac{\sqrt{2\gamma_e}}{p} \right]^{-\beta-2} \left( \frac{\phi}{M_P} \right)^{-\beta-2}, \quad (62)$$

whereas the two other relevant flow parameters  $s$  and  $\eta$  are given by

$$s(\phi) = \frac{2\beta}{p} \epsilon(\phi), \quad (63)$$

$$\eta(\phi) = \frac{p-2}{p} \epsilon(\phi), \quad (64)$$

where we have used (6b), the first expression of (7), plus (33b), (59) and (61). The expression for the number of e-folds is obtained from expressions (38), (39) and (42) for  $\alpha \neq 0$ , so that

$$N(\phi) = \frac{p}{2(\beta+2)} \left[ \frac{1}{\epsilon(\phi)} - 1 \right]. \quad (65)$$

In the analysis performed above we have considered solely models with  $\alpha < 0$  and  $\beta > 0$ ; the case  $\alpha = 0$  has been studied in the paper [21], and leads to potentials like (60) in the  $UV$  limit  $s < 0$ . The case  $\beta = 0$ ,  $\gamma_e = 1$ , corresponds to canonical large-field models; in this limit, the expressions for the flow parameters  $\epsilon$  and  $\eta$ , given by (62) and (64), give

$$\epsilon(\phi) = \frac{p^2 M_P^2}{2 \phi^2}, \quad (66)$$

$$\eta(\phi) = \frac{p(p-2)}{2} \frac{M_P^2}{\phi^2}, \quad (67)$$

which coincides with the results in section III.A of reference [23]. Also in this limit, from (61) we see that inflation ends when

$$\frac{\phi_e^c}{M_P} = \frac{p}{\sqrt{2}}, \quad (68)$$

which coincides with the analogous expression found in [23]<sup>2</sup>. Hence, *all* large-field polynomial models with  $p > 2$  are particular cases of this non-canonical version. Also, if  $\gamma_e \neq 1$ , we recover the Spalinski model [20] with a polynomial potential as well. Another particular case of this general class is *isokinetic inflation*, proposed in [22]. For this model, we can show that by setting  $\alpha = -p/2 - 1$  and  $\beta = p/2 - 1$ , we reproduce all the expressions derived in [22] up to a redefinition of the exponent of the potential<sup>3</sup>.

Therefore, we have a completely well-defined D-brane inflationary scenario with large-field potentials like (60), a flow parameter  $\epsilon$  given by (33a) with  $\alpha < 0$ , and a small speed of sound characterized by (33b) with  $\beta \geq 0$ , reproducing not only the canonical large-field polynomial potentials, but also other models discussed in the literature. For these reasons we will call this class *non-canonical large-field polynomial models*.

In particular, as we will see in section VI, these models predict values for the scalar spectral index and tensor-to-scalar ratio which agree very well with WMAP5 observations.

## B. Small-field polynomial potentials

Small-field polynomial potentials in canonical inflation arise from a spontaneous symmetry breaking in the presence of a “false” vacuum in unstable equilibrium with nonzero vacuum energy density and a “physical” vacuum,

for which the classical expectation value of the scalar field is nonzero,  $\langle \phi \rangle \neq 0$  [30]. These models are characterized by an effective symmetry-breaking scale  $\mu \propto \langle \phi \rangle$  such that  $\phi \ll \mu \ll M_P$ , the field rolls down from an unstable equilibrium at the origin toward  $\mu$ ; hence, for positive  $\phi$  we have always  $\dot{\phi} > 0$ .

For non-canonical models we can express the small-field limit  $\phi \ll \mu$  by choosing  $\alpha > 0$ ; also, as we have derived in section IV C, the condition  $\dot{\phi} > 0$  for  $\phi > 0$  is satisfied when  $\sigma = -1$  and  $\alpha + \beta + 2 > 0$ , which corresponds to the model 5 in table III. In this case, the Hubble parameter (48) takes the form

$$H(\phi) = \tilde{H}_e \exp \left[ -\frac{K \phi_e}{\alpha + \beta + 2} \bar{\phi}^{(\alpha + \beta + 2)/2} \right]; \quad (69)$$

where  $K$  and  $\phi_e$  are given by (50); since  $\bar{\phi} = \phi/\phi_e$  in the small-field limit, and  $\alpha + \beta + 2 > 0$ , we can expand expression (69) to first-order in  $\bar{\phi}$ , so that

$$H(\phi) = \tilde{H}_e \exp \left[ 1 - \frac{K \phi_e}{\alpha + \beta + 2} \bar{\phi}^{(\alpha + \beta + 2)/2} \right]. \quad (70)$$

Since  $\beta > -2 - \alpha$  and  $\alpha > 0$ , we see that  $\beta$  can take either sign; in particular, for  $\beta > 0$ , from (33b) we have the following relation

$$\gamma(\phi) = \gamma_e \left( \frac{\phi}{\phi_e} \right)^{-|\beta|} \implies \gamma \rightarrow \infty \quad \text{as} \quad \phi \rightarrow 0, \quad (71)$$

or, in terms of the speed of sound,

$$c_s \rightarrow 0 \quad \text{as} \quad \phi \rightarrow 0. \quad (72)$$

In the small-field limit, we have always  $\phi \ll \phi_e$ , so that  $\phi \rightarrow 0$  corresponds to early times; then, from (72) we conclude that the field propagates with subluminal speed of sound at early times. Also, property (71) implies that  $\gamma/(\gamma + 1) \rightarrow 1$ , so that by using this fact and plugging (70) into (14), we find

$$V(\phi) \sim 3M_P^2 \tilde{H}_e^2 \left[ 1 - \frac{2}{3} \bar{\phi}^\alpha - \frac{2K \phi_e}{\alpha + \beta + 2} \bar{\phi}^{(\alpha + \beta + 2)/2} \right] \quad (73)$$

in the slow-roll limit. It is clear that we can derive out of expression (73) different sort of potentials, depending on the relations between the exponents. Let us analyze one of such possible choices; we define first the exponent

$$p = \frac{\alpha + \beta + 2}{2}, \quad (74)$$

and we choose  $\alpha$  and  $\beta$  such that  $p$  is always *integer*. Then, if  $\alpha \geq p$ , we see that  $\alpha \geq \beta + 2$ , and the potential (73) takes the form

$$V(\phi) \sim 3M_P^2 \tilde{H}_e^2 \left[ 1 - \frac{K \phi_e}{p} \bar{\phi}^p \right], \quad \alpha \geq \beta + 2. \quad (75)$$

In the canonical small-field scenario the initial unstable equilibrium state is characterized by the vacuum energy

<sup>2</sup> Our notation differs from that adopted in [23]; our  $M_P$  is related to  $m_{pl}$  in that reference by  $M_P = m_{pl}/\sqrt{8\pi}$ .

<sup>3</sup> In isokinetic inflation the potential has the form  $V(\phi) \propto \phi^{2p_{iso}}$  [22], whereas in our model we have defined the exponent  $p$  (expression (44)) such that  $V(\phi) \propto \phi^p$ . Then  $p = 2p_{iso}$ .

density  $\Lambda^4$ , which is the height of the potential at the origin,  $\Lambda^4 = V(0)$ , whereas the effective symmetry-breaking scale is given by [30]

$$\mu = \left[ \frac{(m-1)!V(\phi)}{|d^m V/d\phi^m|} \right]^{1/m} \Big|_{\phi=0}, \quad (76)$$

where  $m$  is the order of the lowest nonvanishing derivative of the potential at the origin. In the non-canonical case, the vacuum energy density is given by

$$\Lambda^4 = 3M_P^2 \tilde{H}_e^2, \quad (77)$$

whereas the effective symmetry-breaking scale (76) reads

$$\frac{1}{\mu^p} = \sqrt{\frac{2\gamma_e}{M_P^2 \phi_e^{\alpha+\beta}}}, \quad (78)$$

then, in terms of these two quantities, the inflationary potential (73) becomes, in the small-field limit,

$$V(\phi) = \Lambda^4 \left[ 1 - \frac{1}{p} \left( \frac{\phi}{\mu} \right)^p \right], \quad (79)$$

as expected. Then, in the non-canonical case the field also rolls down from an unstable vacuum state whose energy density is given by (77) with very low speed of sound, and evolves toward a minimum characterized by a scale  $\mu$  given by (78) for  $\alpha \geq p \geq 2$ , and such behavior is exactly the same as the canonical case.

From (78) we see that inflation ends when

$$\frac{\phi_e}{\mu} = \left[ \frac{\mu}{M_P} \sqrt{2\gamma_e} \right]^{1/(p-1)}, \quad (80)$$

so that the flow parameters are given by

$$\epsilon(\phi) = \left[ \frac{M_P}{\mu \sqrt{2\gamma_e}} \right]^{(p-1)/\alpha} \left( \frac{\phi}{\mu} \right)^\alpha, \quad (81)$$

$$s(\phi) = -\beta \sqrt{\frac{2M_P^2}{\gamma_e \phi_e^2}}, \quad (82)$$

$$\eta(\phi) = (\alpha + \beta) \sqrt{\frac{M_P^2}{2\gamma_e \phi_e^2}} \bar{\phi}^{(\alpha-\beta-2)/2} + \epsilon(\phi), \quad (83)$$

where we have used (6b), the first expression of (7), plus (33a), (33b), (69) and (80).

In particular, in the canonical limit  $\beta = 0$ ,  $\gamma_e = 1$  we have  $\alpha \geq 2$ , so that for *even* values of  $\alpha$  all the potentials with  $p \geq 2$  are reproduced. In this limit, from (74) we see that  $\alpha = 2(p-1)$ ; then, from (81) the flow parameter  $\epsilon$  assumes the form

$$\epsilon(\phi) = \frac{M_P}{\mu \sqrt{2}} \left( \frac{\phi}{\mu} \right)^{2(p-1)}, \quad (84)$$

whereas from (80) we see that inflation ends at

$$\frac{\phi_e}{\mu} = \left[ \frac{\mu}{M_P} \sqrt{2} \right]^{1/(p-1)}. \quad (85)$$

Expressions (84) and (85) agree with the corresponding expressions (3.25) and (3.26) in [30] derived for canonical small-field potentials.

Therefore, in the slow-roll limit *all* canonical small-field polynomial models with  $p \geq 2$  are particular solutions to the non-canonical model described in this section when  $\beta = 0$ ,  $\gamma_e = 1$  and  $\alpha$  even; hence, we have again a well-defined D-brane inflationary scenario with a small-field potential like (79), a flow parameter  $\epsilon$  given by (33a) with  $\alpha > 0$ , and a small speed of sound characterized by (33b) with  $\beta \leq 0$ , reproducing all the canonical small-field polynomial potentials when  $\beta = 0$ . For these reasons we will call this class *non-canonical small-field polynomial models*.

### C. Hybrid potentials

In the last two sections we have discussed the small-field models characterized by  $\dot{\phi} > 0$  for positive  $\phi$ , given by the model 5 in table III. Let us now examine a similar model, with  $\alpha + \beta + 2 > 0$  but with  $\dot{\phi} < 0$  for positive  $\phi$ . In this case,  $\sigma = +1$ , (model 6 in table III); then, the Hubble parameter (48) takes the form

$$H(\phi) = \tilde{H}_e \exp \left[ \frac{K \phi_e}{\alpha + \beta + 2} \bar{\phi}^{(\alpha+\beta+2)/2} \right], \quad (86)$$

where the constant  $K$  and variable  $\bar{\phi}$  are given by the definitions (50). Since  $\bar{\phi} \ll 0$  and  $p > 0$ , where  $p$  is given by (74), we expand expression (86) to first-order in  $\bar{\phi}$ ,

$$H(\phi) = \tilde{H}_e \exp \left[ 1 + \frac{K \phi_e}{2p} \bar{\phi}^p \right]. \quad (87)$$

The analysis leading to the sign of  $\beta$  is identical to that made in section VB since, as in that case,  $\beta > -2 - \alpha$  and  $\alpha > 0$ ; then, using the same arguments we find that the field rolls down the potential with a subluminal speed of sound. Also, since  $\gamma/(\gamma+1) \rightarrow 1$  at early times, we have, plugging (87) into (14), that

$$V(\phi) \sim 3M_P^2 \tilde{H}_e^2 \left[ 1 - \frac{2}{3} \bar{\phi}^\alpha + \frac{K \phi_e}{p} \bar{\phi}^p \right] \quad (88)$$

in the slow-roll limit. As in the model derived in section VB, we choose  $\alpha$  and  $\beta$  such that  $p$  is always integer; then, for  $\alpha > p$ , the potential (88) takes the form

$$V(\phi) \sim 3M_P^2 \tilde{H}_e^2 \left[ 1 + \frac{K \phi_e}{p} \bar{\phi}^p \right]. \quad (89)$$

In this case, the minimum of the potential is at the origin, as in the small-field polynomial case, but now  $V(\phi) >$



$V(0)$  around  $\phi = 0$ . Therefore, the field rolls toward the minimum with nonzero vacuum energy,  $\Lambda^4 = V(0)$ . This is exactly the behavior of the canonical hybrid potentials [32, 33]. Then, we may write the potential (86) as

$$V(\phi) \sim \Lambda^4 \left[ 1 + \left( \frac{\phi}{\mu} \right)^p \right], \quad (90)$$

where we have defined

$$\frac{1}{\mu^p} = \frac{1}{p} \sqrt{\frac{2\gamma_e}{M_P^2 \phi_e^{2(p-1)}}}. \quad (91)$$

#### D. Exponential potentials

Along with the models discussed above, there is a fourth type whose Hubble parameter and potential are exponentials [23]. Since the general expression for the Hubble parameter derived in section IV C is of an exponential form, we focus on its large-field limit solution, given by the model 4 in table II. In this case  $\dot{\phi} < 0$  for positive  $\phi$ , so that  $\sigma = +1$ . The expression for the Hubble parameter (48) for  $\alpha < 0$ , is given by

$$H(\phi) = \tilde{H}_e \exp \left[ \sqrt{\frac{1}{2p}} \left( \frac{\phi}{M_P} \right)^{\alpha+\beta+2} \right], \quad (92)$$

where we have defined

$$p = \frac{(\alpha + \beta + 2)^2}{4\gamma_e} \left( \frac{\phi_e}{M_P} \right)^{\alpha+\beta}. \quad (93)$$

Since  $\alpha + \beta + 2 > 0$ , the exponent of the speed of sound is restricted to the values  $\beta > -\alpha - 2$ ; then, for  $\beta > 0$ , we have that  $\gamma \rightarrow \infty$  as  $\phi \rightarrow \infty$ , and then  $c_s \rightarrow 0$  at early times since  $\phi$  is in the large-field limit. Hence, the field propagates with a subluminal speed of sound at early times, and  $\gamma/(\gamma + 1) \rightarrow 1$ . Using this fact and substituting (92) into (14) we find

$$V(\phi) \sim 3M_P^2 \tilde{H}_e^2 \exp \left[ \sqrt{\frac{2}{p}} \left( \frac{\phi}{M_P} \right)^{\alpha+\beta+2} \right]. \quad (94)$$

Then, the field rolls down the potential toward the minimum at origin, characterized by a nonzero vacuum energy  $V(0) = \Lambda^4$  with a subluminal speed of sound. This is similar to the behavior of exponential potentials in canonical models, except for the fact that  $c_s = 1$ . Since  $\Lambda^4 = 3M_P \tilde{H}_e^2$ , the final form of the non-canonical potential (94) is

$$V(\phi) \sim \Lambda^4 \exp \left[ \sqrt{\frac{2}{p}} \left( \frac{\phi}{M_P} \right)^{\alpha+\beta+2} \right]. \quad (95)$$

Before we study the non-canonical limit of the potential (95), let us have a look first at the flow-parameter

$\epsilon$ . We have used the parametrization associated with  $\alpha \neq 0$ , given by (33a), but we can make it general as follows: substituting and (33b) and (93) into (33a), we find

$$\epsilon(\phi) = \frac{(\alpha + \beta + 2)^2}{4p\gamma(\phi)} \left( \frac{\phi}{M_P} \right)^{\alpha+\beta}. \quad (96)$$

which holds even when  $\alpha = 0$ , for  $\epsilon(\phi) = \epsilon = \text{const.}$  in that case. The other two flow parameters  $s$  and  $\eta$  are given respectively by

$$s(\phi) = \beta \left( \frac{\phi}{M_P} \right)^{-1} \sqrt{\frac{2\epsilon(\phi)}{\gamma(\phi)}}, \quad (97)$$

$$\eta(\phi) = \frac{\alpha + \beta}{\sqrt{2}} \left( \frac{\phi}{M_P} \right)^{-1} \sqrt{\frac{\epsilon(\phi)}{\gamma(\phi)}} + \epsilon(\phi), \quad (98)$$

where we have used (6b), the first expression of (7), plus (33b) and (92).

Then, with the parametrization defined by (96), we see that in the canonical case  $\alpha = \beta = 0$ ,  $\gamma_e = 1$ , expressions (96) and (98) give

$$\epsilon(\phi) = \eta(\phi) = \frac{1}{p}, \quad (99)$$

which matches the results derived for the canonical case as shown in [23]. Expression (99) shows that we have to restrict the values of (93) to be  $p > 1$ , so that we get  $\epsilon \leq 1$  in the canonical limit.

Therefore, we have a completely well-defined D-brane inflationary scenario with exponential potentials like (95), a flow parameter  $\epsilon$  given by (96) with  $\alpha \leq 0$ , and a small speed of sound characterized by (33b) with  $\beta \geq 0$ , which reproduces the corresponding canonical model. We will call this class *non-canonical exponential models*.

The four distinct non-canonical classes obtained so far are summarized in Table IV below.

## VI. AN APPLICATION OF NON-CANONICAL LARGE-FIELD POLYNOMIAL MODELS

In this section we study some applications of the large-field models derived in section V A. We choose this class of non-canonical potentials because the expressions for the scalar spectral index, the tensor/scalar ratio and the level of non-gaussianity are particularly simple, depending on two parameters solely,  $p$  and  $\beta$ . Let us first derive an expression for the flow parameter  $\epsilon$  in terms of  $N$ . From (62) and (65) we find

$$\epsilon(N) = \frac{p}{p + 2(\beta + 2)N}. \quad (100)$$

The other two flow parameters  $s$  and  $\eta$  are given by

$$s(N) = \frac{2\beta}{p + 2(\beta + 2)N}, \quad (101)$$

TABLE IV: A summary of the distinct models discussed in this work.

model	$\alpha$	$\beta$	$p$	$V(\phi)$
Large-field	$\alpha = -\beta - 2$	$\beta \geq 0$	$\phi_e \sqrt{\frac{2\gamma_e}{M_P^2}}$ <sup>a</sup>	$\Lambda^4 \left(\frac{\phi}{\mu}\right)^p$
Small-field	$\alpha \geq p$	$\beta \leq 0$	$\frac{\alpha+\beta+2}{2}$ <sup>b</sup>	$\Lambda^4 \left[1 - \frac{1}{p} \left(\frac{\phi}{\mu}\right)^p\right]$
Hybrid	$\alpha \geq p$	$\beta \leq 0$	$\frac{\alpha+\beta+2}{2}$ <sup>c</sup>	$\Lambda^4 \left[1 + \left(\frac{\phi}{\mu}\right)^p\right]$
Exponential	$\alpha \leq 0$	$\beta \geq 0$	$\frac{(\alpha+\beta+2)^2}{4\gamma_e} \left(\frac{\phi_e}{M_P}\right)^{\alpha+\beta}$ <sup>d</sup>	$\Lambda^4 \exp \left[ \sqrt{\frac{2}{p}} \left(\frac{\phi}{M_P}\right)^{\alpha+\beta+2} \right]$

<sup>a</sup>Corresponds to model 1 in table I.

<sup>b</sup> $p$  is integer. Corresponds to model 5 in table III.

<sup>c</sup> $p$  is integer. Corresponds to model 6 in table III.

<sup>d</sup> $p > 1$ . Corresponds to model 4 in table II.

$$\eta(N) = \frac{p-2}{p+2(\beta+2)N}; \quad (102)$$

where we have used (6b), the first expression of (7), plus (33b), (59) and (100). Inserting (100), (101) and (102) into (30), we find, in the slow-roll limit,

$$n_s = 1 - \frac{2(p+2\beta+2)}{p+2(\beta+2)N}. \quad (103)$$

The expression for the speed of sound in terms of  $N$  can be calculated in the same way: we use (33a), (33b) and (65), so that

$$c_s(N) = \frac{1}{\gamma_e} \left[ \frac{p}{p+2(\beta+2)N} \right]^{\beta/(\beta+2)}. \quad (104)$$

Through the use of (31), (100) and (104) we can derive a general expression for the tensor/scalar ratio, which is given by

$$r(N) = \frac{16}{\gamma_e} \left[ \frac{p}{p+2(\beta+2)N} \right]^{2(\beta+1)/(\beta+2)}. \quad (105)$$

The expression for the level of non-gaussianity  $f_{NL}$  is given by [18]

$$f_{NL} = -\frac{35}{108} \left( \frac{1}{c_s^2} - 1 \right), \quad (106)$$

which can be easily evaluated by using expression (104).

Therefore, the tensor/scalar ratio will have a power-law dependence as well, with exponent  $2(\beta+1)/(\beta+2)$ , which means that, for a given value of  $p$ , a larger  $\beta$  corresponds to a smaller  $r$ . Since  $\beta \geq 0$  for non-canonical

large-field models, we have, from (5) and (33b), that  $c_s \propto \phi^{-\beta}$ ; then, fields rolling with *slower* speed of sound would produce *lower* tensor/scalar ratios. However, from (106), we see that  $f_{NL}$  depends on  $c_s^{-2}$ , and then a low speed of sound would produce a *larger* level of non-gaussianity; then, for large-field models low- $r$  tensor modes are strongly correlated with the amplitude of non-gaussianity, as has been discussed in the reference [22] for isokinetic inflation. Then, the suppression of tensor modes by a large amount of non-gaussianity is a feature shared by all non-canonical models with large-field polynomial potentials.

Let us next make some predictions on the values of  $n_s$ ,  $r$  and  $f_{NL}$  through expressions (103), (105) and (106) respectively, when the modes cross the horizon 46 or 60 e-folds before the end of inflation. As we have discussed in section IV A, we have set  $\gamma_e = 1$ , which characterizes the end of inflation; the results are depicted in figures 1 and 2. In both figures, the top left plots refer to the variation of the scalar index in terms of  $\beta$  for each value of  $p$ . The top right plots in Figs. 1 and 2 show the corresponding tensor/scalar ratio. In these plots we see that for larger values of  $p$  and small  $\beta$  the modes have large values of  $r$  (the observable lower bound is  $r < 0.22$ ); then, as  $\beta$  increases, the speed of sound gets lower and, in consequence, the tensor/scalar ratio as well. However, as shown in (106), a field rolling very slowly produces a large amount of non-gaussianity, as can be seen in the bottom left plots of figures 1 and 2. Therefore, as was first discussed in the particular case of isokinetic inflation [22], the production of large non-gaussianity is strictly correlated with low tensor amplitudes, and this is a feature common to all large-field polynomial potentials. This behavior is shown in the bottom right plots of figures 1 and

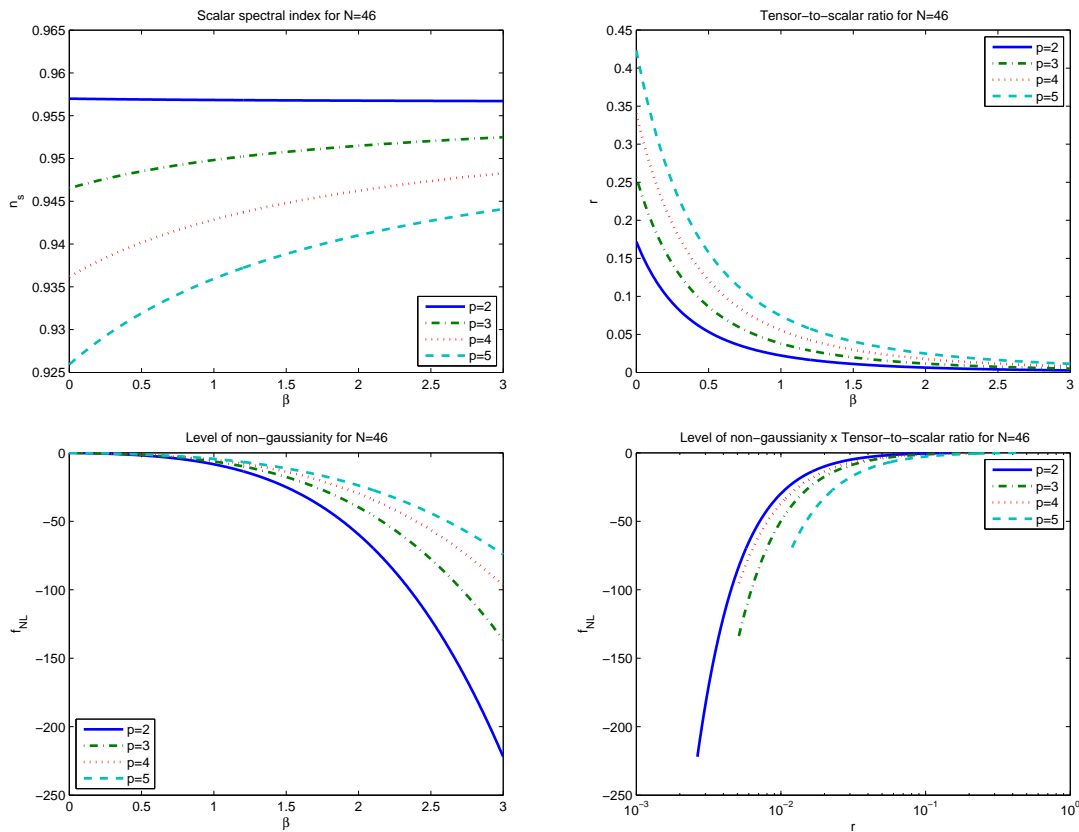


FIG. 1: The observables  $n_s$  (top left),  $r$  (top right) and  $f_{NL}$  (bottom left) as a function of the exponent of the speed of sound  $\beta$  for each value of  $p$  ( $V(\phi) \propto \phi^p$ ) for  $N = 46$ . On bottom right is depicted the behavior of  $f_{NL}$  compared to  $r$ .

2.

We next compare the results obtained with the current WMAP5 data [1], [6]. The results are depicted in Fig. 3 for different values of  $p$ . Straight lines indicate the different values of  $\beta$ , with the left (right) extremity indicating the value of  $(n_s, r)$  evaluated at  $N = 46$  ( $N = 60$ ). As shown in [6], all canonical models with  $p > 2$  are ruled out by WMAP5 data alone; however, in the non-canonical case, figure 3 shows that the models with  $p \leq 5$  are also consistent with the observable data. A field evolving with slow-varying speed of sound produces low-amplitude tensors, then pushing the values  $(n_s, r)$  inwards the observable region. However, a large amount of non-gaussianity is produced, which is a distinct signature of non-canonical large-field polynomial models and can be a powerful observable to discriminate among inflationary models.

## VII. CONCLUSIONS

In this paper we propose a general DBI model characterized by a power-law flow-parameter power-law flow parameter  $\epsilon(\phi) \propto \phi^\alpha$  and speed of sound  $c_s(\phi) \propto \phi^\beta$ , where  $\alpha$  and  $\beta$  are constants. We show that this general model has distinct classes of solutions depending on the

relation between  $\alpha$  and  $\beta$ , and on the time evolution of the inflaton field. These classes of solutions are summarized in tables I, II and III. In particular, we show that in the slow-roll limit the four well-known canonical potentials arise naturally in this general DBI model, having similar properties to their canonical counterparts, except that the speed of sound in general varies with time. We also show that this general DBI model encompasses not only all the canonical models with the mentioned potentials, but other D-brane scenarios as well: the DBI model with constant speed of sound [20], with constant flow parameters [21], and isokinetic inflation [22]. The four non-canonical models are summarized in table IV.

We also derive the expressions for the spectral index, tensor/scalar ratio and the amplitude of non-gaussianity for large-field potentials in the slow-roll limit. We show that a low speed of sound suppresses the tensor/scalar ratio  $r$  and produces a large amount of non-gaussianity, a feature already explored in the case of isokinetic inflation, and shown to be a general property of all large-field DBI models with polynomial potentials. Unlike canonical inflation, where all polynomial models with  $p > 2$  are ruled out, the suppression of tensor modes in the non-canonical version allows a larger class of polynomial potentials to lie within the observable range; also, the production of large amount of non-gaussianity is a distinct signature

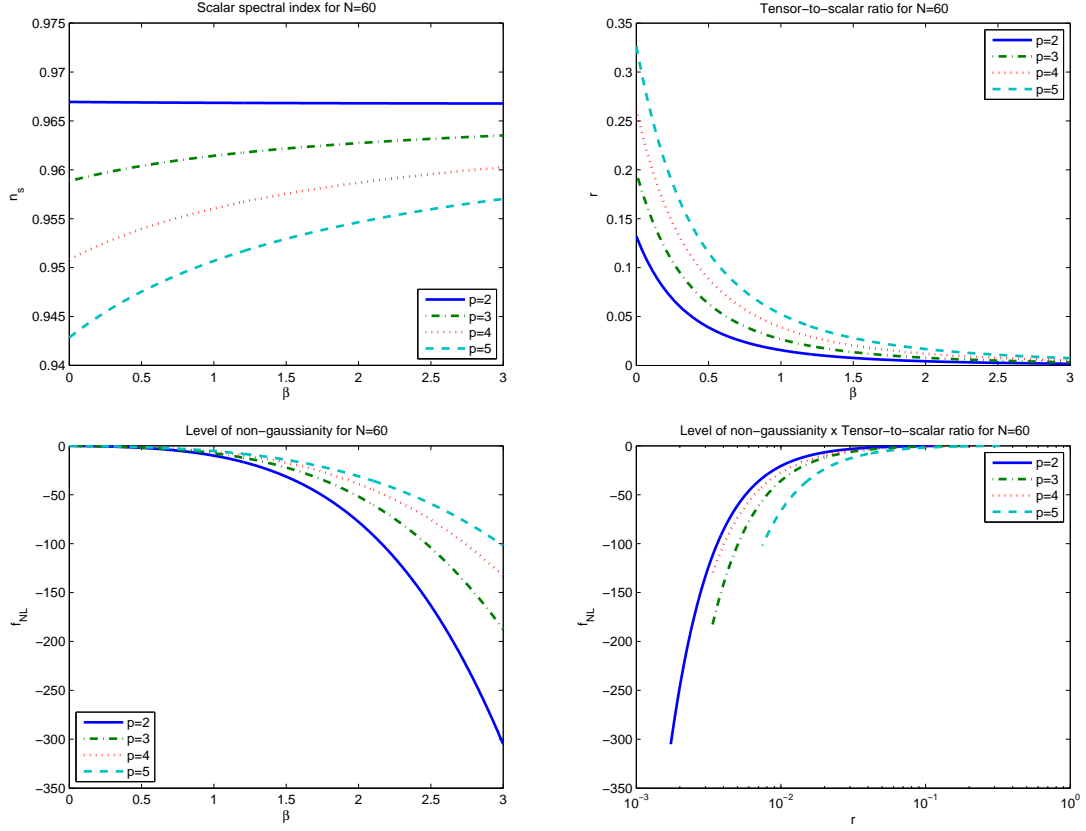


FIG. 2: The observables  $n_s$  (top left),  $r$  (top right) and  $f_{NL}$  (bottom left) as a function of the exponent of the speed of sound  $\beta$  for each value of  $p$  ( $V(\phi) \propto \phi^p$ ) for  $N = 60$ . On bottom right is depicted the behavior of  $f_{NL}$  compared to  $r$ .

of these DBI large-field models, which can be a powerful observable to discriminate among inflationary models.

### Acknowledgments

DB thanks Brazilian agency CAPES for financial support. This research is supported in part by the National

Science Foundation under grant NSF-PHY-0757693.

- 
- [1] E. Komatsu *et al*, *Astrophys. J. Suppl.Ser.*, **180**, 330 (2009)
  - [2] A. A. Starobinskiĭ, *JETP Lett.*, **30**, 682 (1979)
  - [3] A. H. Guth, *Phys. Rev. D* **23**, 347 (1981).
  - [4] A. D. Linde, *Phys. Lett. B* **108**, 389 (1982).
  - [5] A. Albrecht and P. J. Steinhardt, *Phys. Rev. Lett.* **48**, 1220 (1982).
  - [6] W. H. Kinney, E. W. Kolb, A. Melchiorri, & A. Riotto, *Phys. Rev. D* **78**, 087302 (2008) [arXiv:0805.2966].
  - [7] S. Kachru, R. Kallosh, A. Linde, J. M. Maldacena, L. McAllister and S. P. Trivedi, *JCAP* **0310** (2003) 013 [arXiv:hep-th/0308055].
  - [8] J. J. Blanco-Pillado *et al.*, *JHEP* **0411**, 063 (2004) [arXiv:hep-th/0406230].
  - [9] J. R. Bond, L. Kofman, S. Prokushkin and P. M. Vaudrevange, *Phys. Rev. D* **75**, 123511 (2007) [arXiv:hep-th/0612197].
  - [10] E. Silverstein and D. Tong, *Phys. Rev. D* **70**, 103505 (2004) [arXiv:hep-th/0310221].
  - [11] C. Armendariz-Picon, T. Damour and V. F. Mukhanov, *Phys. Lett. B* **458**, 209 (1999) [arXiv:hep-th/9904075].
  - [12] M. Alishahiha, E. Silverstein and D. Tong, *Phys. Rev. D* **70**, 123505 (2004) [arXiv:hep-th/0404084].
  - [13] X. Chen, M. X. Huang, S. Kachru and G. Shiu, *JCAP* **0701**, 002 (2007) [arXiv:hep-th/0605045].
  - [14] M. Spalinski, *Phys. Lett. B* **650**, 313 (2007) [arXiv:hep-th/0703248].
  - [15] R. Bean, X. Chen, H. V. Peiris and J. Xu, *Phys. Rev. D*, **77**, 023527 (2008) arXiv:0710.1812 [hep-th].
  - [16] M. LoVerde, A. Miller, S. Shandera and L. Verde, *JCAP*,

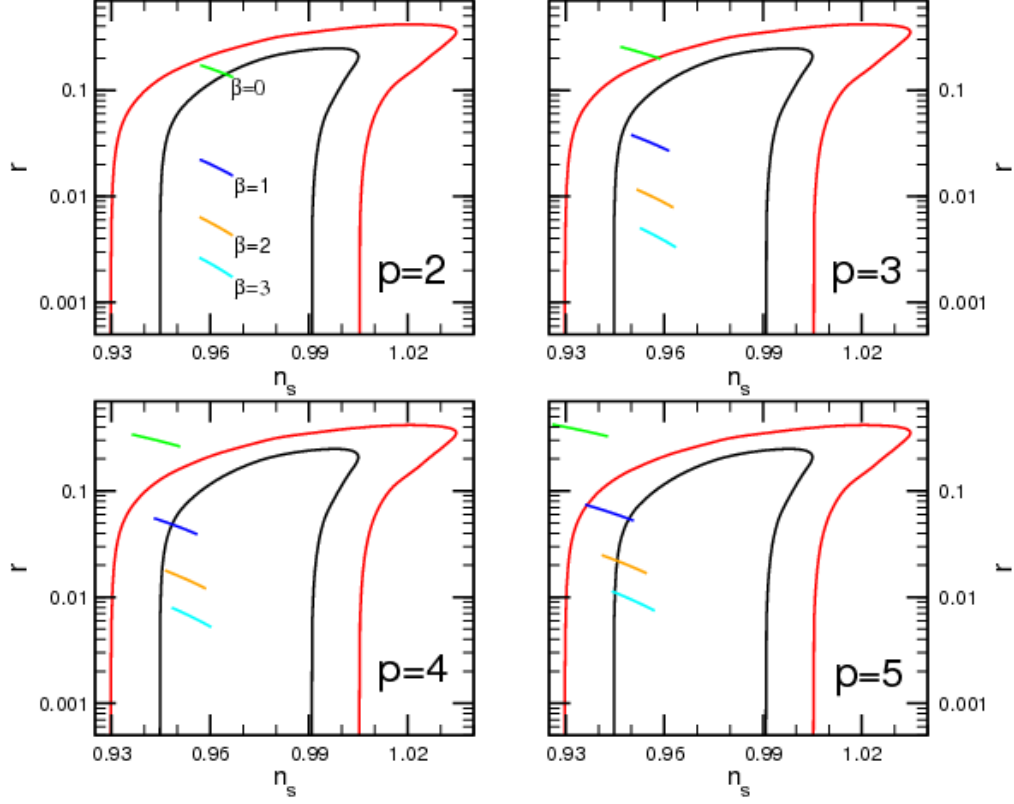


FIG. 3: 68 % (black) and 95 % C.L. (red) on the  $n_s$  and  $r$  parameter space for WMAP5 alone. In each panel we plot the values of  $n_s$  and  $r$  for a specific potential  $V(\phi) \propto \phi^p$  according to the exponent  $\beta$  of the speed of sound. Green lines correspond to  $\beta = 0$  (canonical limit), blue lines to  $\beta = 1$ , orange lines to  $\beta = 2$  and light blue lines to  $\beta = 3$ . The left (right) extremity of each line correspond to the case where a mode crossed the sound horizon 46 (60) e-folds before the end of inflation.

- 4, 14 (2008) [arXiv:0711.4126 [astro-ph].
- [17] W. H. Kinney, Phys. Rev. D **66**, 083508 (2002) [arXiv:astro-ph/0206032].
- [18] H. V. Peiris, D. Baumann, B. Friedman and A. Cooray, Phys. Rev. D **76**, 103517 (2007) [arXiv:0706.1240 [astro-ph]].
- [19] L. P. Chimento and R. Lazkoz, Gen. Rel. and Grav. **40**, 2543 (2008) [arXiv:0711.0712 [hep-th]].
- [20] M. Spalinski, JCAP **4**, 2 (2008) [arXiv:0711.4326].
- [21] K. Tzirakis and W. H. Kinney, Phys. Rev. D **77**, 010 (2008) [arXiv:0712.2043].
- [22] K. Tzirakis and W. H. Kinney, JCAP **01**, 028 (2009) [arXiv:0810.0270].
- [23] S. Dodelson, W. H. Kinney and E. W. Kolb, Phys. Rev. D **56**, 3207 (1997) [arXiv:astro-ph/9702166].
- [24] L. McAllister and E. Silverstein, Gen. Rel. Grav. **40**, 565 (2008) [arXiv:0710.2951 [hep-th]].
- [25] J. M. Cline, arXiv:hep-th/0612129.
- [26] I. R. Klebanov and M. J. Strassler, JHEP **0008**, 052 (2000) [arXiv:hep-th/0007191].
- [27] M. Spalinski, JCAP **0704**, 018 (2007) [arXiv:hep-th/0702118].
- [28] J. Garriga and V. F. Mukhanov, Phys. Lett. B **458**, 219 (1999) [arXiv:hep-th/9904176].
- [29] S. E. Shandera and S. H. Tye, JCAP **0605** (2006) 007 [arXiv:hep-th/0601099].
- [30] W. H. Kinney and K. T. Mahanthappa, Phys. Rev. D **53**, 5455 (1996) [arXiv:hep-ph/9512241].
- [31] K. Freese, J. A. Frieman and A. V. Olinto, Phys. Rev. Lett. **65** (1990) 3233.
- [32] A. D. Linde, Phys. Lett. B **259** (1991) 38.
- [33] A. D. Linde, Phys. Rev. D **49**, 748 (1994) [arXiv:astro-ph/9307002].